

Dynamic Surfaces

Simon Salamon

Abstract After discussing some well-known examples in geometry and function theory, we study surfaces in space that are defined by the vanishing of the torsion of integral curves of a given vector field.

1 Introduction

This is a record of a lecture given at the ESMA conference on mathematics and art at the Institut Henri Poincaré in Paris on 20 July 2010. The aim was to present a number of striking images and animations based on the application of techniques from both differential geometry and dynamical systems. This article retains the title of the lecture, even though it can only present still images; the true dynamic content can be found from links in the references at the end of the article.

A typical example is the opaque surface visible in Fig. 1 "supporting" the celebrated Lorenz attractor. The surface consists of points in space at which the corresponding trajectory has zero torsion, a concept that will be intuitively described in Sect. 3 and that is defined in any elementary course on the differential geometry of space curves. Yet the surface is defined by an extremely complicated equation of degree 8 (reproduced as Fig. 12), whose significance could not be recognized without the underlying theory. Like the study of fractals, this is primarily based on scientific discovery, but the cataloguing of the resulting images has an artistic aspect to it. The point of this article is to give a glimpse of both the theory and the imagery to a wide audience.

To introduce the subject of differential geometry that underlies the approach, Fig. 2 is the author's photograph of part of a lecture by Richard Hamilton in Pisa in 2004. Whilst the blackboard relayed advanced mathematics to an expert audience

S. Salamon (✉)

Politecnico di Torino, Corso Duca degli Abruzzi 24, 10129 Torino, Italia
e-mail: salamon@calvino.polito.it

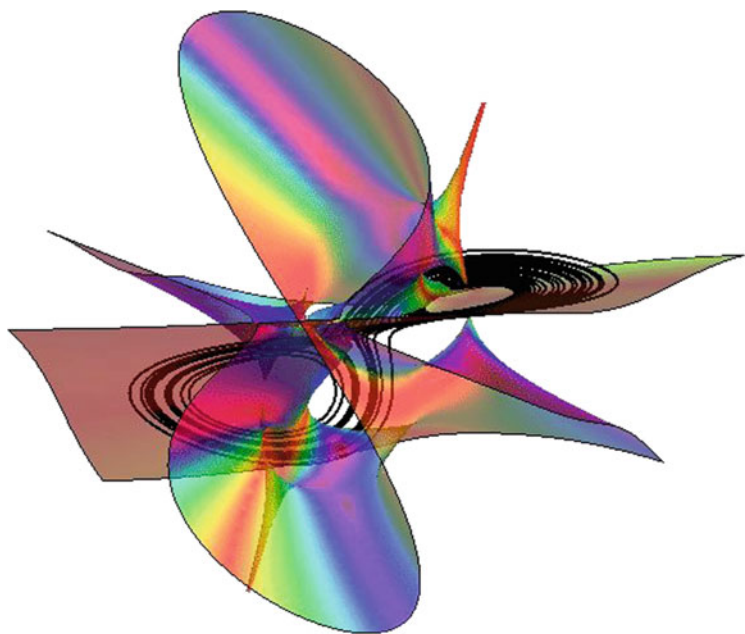


Fig. 1 Lorenz surface

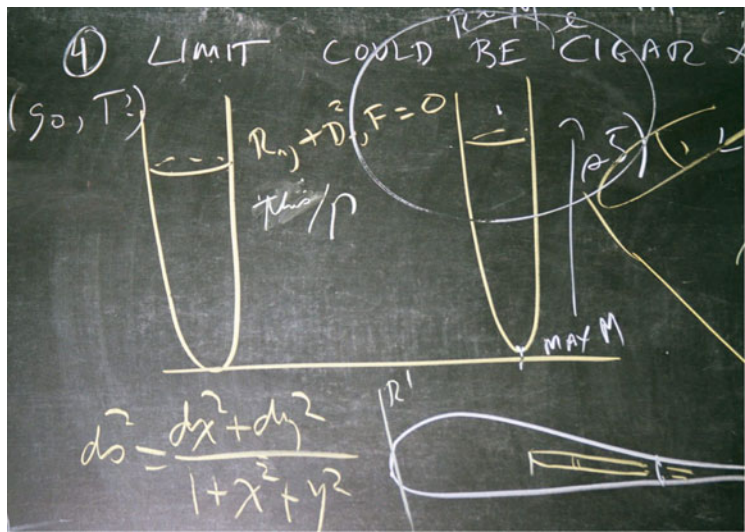


Fig. 2 Discussion of Ricci flow

of conference participants, it conveys even now the essence of mathematical communication carried out part sketching and part symbolizing.

The significant nature of the particular subject is not in question. The original method that the lecturer was describing formed the basis for the proof of the Poincaré conjecture that was confirmed by the offer of a Fields Medal to Gregori Perelman in 2006. It is

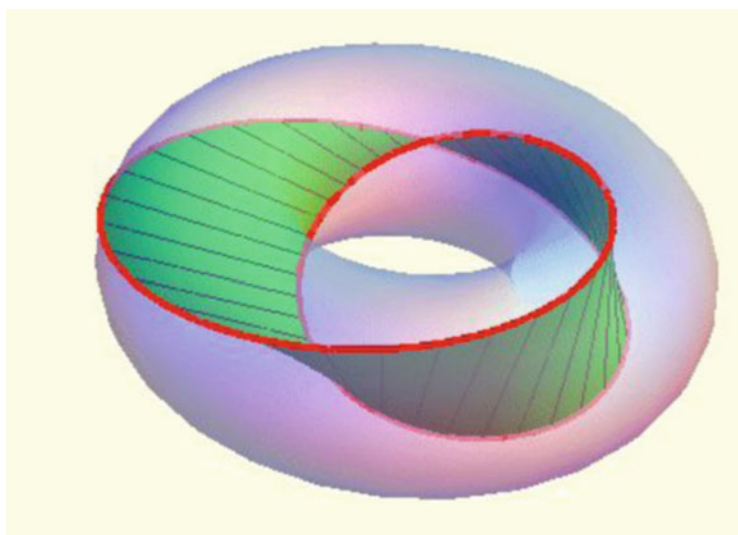


Fig. 3 A band in a torus

based on the concept of Ricci flow, concerning trajectories like the looping black curve in Fig. 1 but in a much more abstract space of tensors. As for the sketches, the reader can judge to what extent these are artistic, but there is no doubt that they reflect the creative nature of the geometric arguments involved and the extent to which contemporary mathematics naturally blurs the distinction between creativity and discovery.

The discussion, diagrammatic and otherwise, concerns the evolution of mathematical objects in time as described by differential equations, one of which is clearly visible in the top centre of Fig. 2. The first term in this equation is the so-called Ricci curvature tensor, R_{ij} , that features in Einstein's formulation of general relativity, but is here used to measure the distortion of a 3-dimensional object. At a more mundane level, it generalizes the description one can give of the convexity or concavity of a surface in space (like the ones in Figs. 1 and 3). The fourth temporal dimension is represented by the horizontal line.

Experts will recognize other main themes in Fig. 2, namely (bottom left) a simple Riemannian metric ds^2 in two isothermal variables x, y that represents the geometry of a surface, and the concept of a discrete quotient ("*this/G*"), which is used by mathematicians to describe an everyday object like a torus. A more concrete version of the latter is the opaque doughnut-shaped surface visible in Fig. 3 housing a Möbius band whose red boundary is a knot on the torus surface.

2 Creativity Versus Discovery

As its name suggests, differential geometry combines the use of differential calculus with the description of geometrical objects. It grew out of more conventional analysis in which geometrical ideas abound, for example recognizing a function by

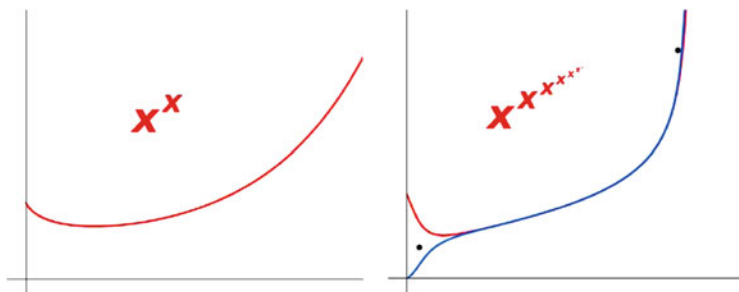


Fig. 4 Three graphs

means of its graph. We shall illustrate this idea with the well-known example of iterated exponentiation in which it is hard to deny some element of creativity amidst the scientific journey of discovery that began with Euler in the 1700s, and continues to fascinate both amateur and professional mathematicians.

We begin by plotting (in Fig. 4 left, though not quite to scale) what is visually one of the simplest looking functions, namely $y = x^x$, chosen for the very economy of notation with which one indicates the operation of exponentiation. The subsequent images on this and the next page refer to repeating this exponential process. By turning the handle just a few times, one obtains a sequence of graphs like the two in Fig. 4 right that combines the plots of eight x 's (red) and nine x 's (blue) arranged in so-called "power towers".

As we take more and more x 's, one can experimentally verify a theorem of Euler, namely that if the tower is continued ad infinitum, it approaches a definite limit precisely when

$$e^{-e} \leq x \leq e^{1/e},$$

the extreme points of convergence left and right being indicated by black dots. A modern proof relies on the contraction mapping theorem and the continuity method. The limit function (that one can imagine extending between the black dots) is in fact the inverse function of $x^{1/x}$. (Graphically, the two functions are mirror images in the diagonal graph $y = x$, whilst experts will know that the inverse can be expressed in terms of the Lambert w function.) With the power of today's personal computers, it is easy to discover this phenomenon for oneself.

The appearance of a bifurcation around the left black dot in Fig. 4 right is inevitable since, as x tends to zero, the graph tends to 1 for an even number of x 's, but to 0 for an odd number of x 's. Euler tells us that the divergence occurs when x is about 0.03. After extending the graphs of Fig. 4 to the left of the vertical axis and into three dimensions with the aid of complex numbers, one soon discovers two trifurcation points, where the graph divides into three branches. The extended 3-dimensional graph is displayed in Fig. 5 (in which a brown line corresponds to the vertical axes of Fig. 4) whose horizontal scale has been exaggerated.

Fig. 5 Bifurcation leading to two trifurcations

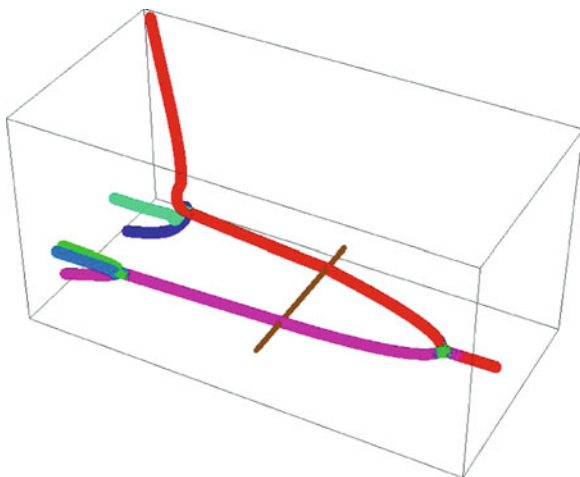
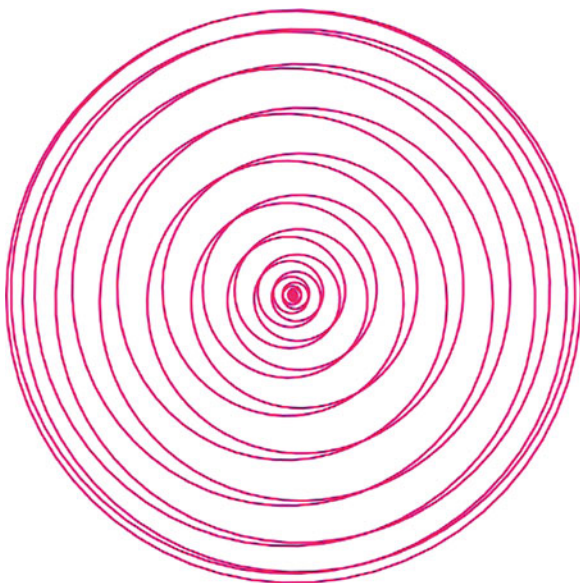


Fig. 6 A hidden spiral



In fact the two tripod legs on the left of Fig. 5 already house some surprises, like many slim helices that project to spirals of the type shown in Fig. 6. This one is thousands of times off the scale of Fig. 5, which illustrates period doubling and tripling familiar in other discrete dynamical processes.

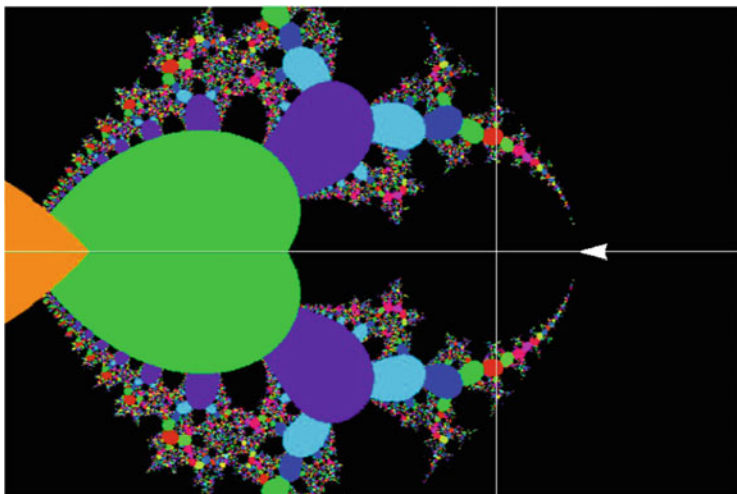


Fig. 7 Exponential convergence

Following the flow of the vessels beyond the left edge of the box in Fig. 5, we are soon led to the onset of chaos. An incomplete fractal picture is illustrated as Fig. 7, in which the bifurcation point corresponds to the tip of the white arrow. It incorporates geometrical tell-tale signs of the convergence theory of iterated functions, such as the cardioid shape familiar from the analogous set of Mandelbrot.

One can think of Fig. 7 as the floor plan associated to a video game; at the bifurcation point one is abandoning Euler's interval of certain convergence for the duality inherent in the second stage that takes place in the first almost-circular chamber. The triple forking occurs at the next doorway at the centre of the overall black rectangle. Soon after that, quantum-like effects occur as gems that are to be plucked out of the air for extra points, though their presence goes unnoticed on the accompanying low-resolution images. Such gems include various spirals; the one in Fig. 6 could with hindsight be drawn with a simple mathematical formula using the techniques of [3], though it is actually the genuine object that was plotted by computer with exponential iteration.

3 Serret-Frenet Geometry

The previous section was designed to show how a simple mathematical idea can quickly lead to objects of aesthetic value. However, the main theme of the lecture concerned the construction of surfaces related to space curves and vector fields. We shall discuss the former in this section and the latter in the next. A space curve is

formed by the trajectory of a particle (or a small flying insect) in space. As such it is described by a triple

$$(x(t), y(t), z(t))$$

of three functions of an independent variable t . We usually suppose that the curves are "smooth" (technically speaking, the three functions of t must be differentiable several times).

Whilst t can be thought of as time, it is better to make use of a different variable, denoted s , that represents arc-length measured along the curve. This is a natural parameter that is uniquely specified by the curve (independently of how it is traced) and a starting point (that we take to correspond to $s = 0$); if the curve were a piece of cotton, it would suffice to pull it tight and measure its length from the anchored starting point.

Mathematically it is known that any curve in space can be completely described by two functions of arc-length: the so-called *curvature* $K(s)$ and *torsion* $\tau(s)$, traditionally indicated by Greek letters. Once these are assigned, they determine the curve up to a rigid motion: there is a unique one, once we assign an initial point and an initial direction for the curve to be tangent to. For example, the curve in Fig. 8 corresponds to

$$\kappa(s) = s \cos s, \quad \tau(s) = \log s,$$

starting from $s = 1$ (the straighter part on the left). This figure illustrates the significance of curvature and torsion, which we explain next.

The curvature of a point in the plane measures the bending of the curve at that point. More precisely, it is equal to the rate of change of the angle between

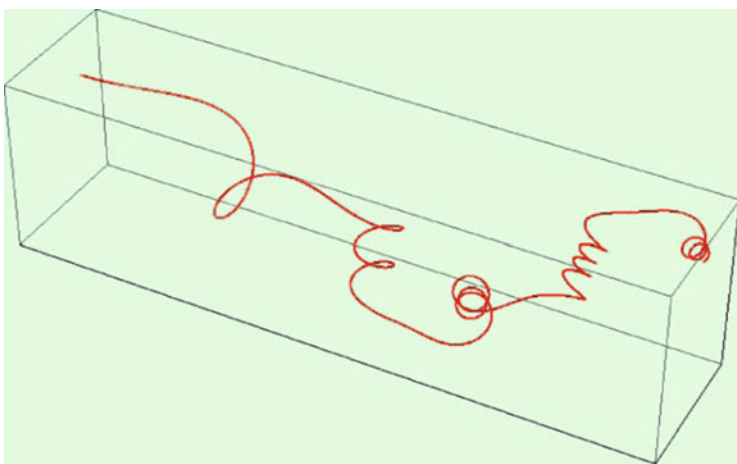


Fig. 8 A space curve with assigned curvature and torsion

the tangent line to the curve and a fixed direction. When the curve is a circle of radius r , the bending is the same at any point of the circle, and the curvature assumes the constant value $1/r$. In this sense, curvature equals the reciprocal of radius.

By taking plane sections of surfaces, one can discuss the curvature of a surface relative to any tangent direction and the maximum and minimum values of this function have special significance. Their product is the so-called Gaussian curvature that is generalized by the tensors of Ricci and Riemann, the basis for measuring the curvature of space-time in General Relativity. Positive Gaussian curvature at a point indicates that the surface is bending away entirely to one side of its tangent plane, and represents convexity at that point.

A similar definition applies to the curvature of a space curve. Once one has specified a point of the curve by assigning the value of s , then $K(s)$ equals $1/r$, where r is the radius of the circle that best fits the curve at that point. A circle is a very special sort of space curve not just because its curvature is constant but because (as a consequence) it always lies in some plane. In general, the fit of a circle to a space curve at a given point can only be approximate, though one can prove that there is a best fit (the "osculating" or "kissing" circle). In Fig. 8, the curve has alternating straight and curly segments since $s \cos s$ is oscillatory and keeps returning to zero. But the amplitude of its peaks becomes greater and greater, so the curly interludes become more pronounced as one moves to the right.

The only setback for space curves is that there is no way of assigning a sign to the curvature function K which therefore (like the mass of an object) takes only non-negative values. By contrast, the torsion of a space curve has a definite sign that is best appreciated by considering a helix. As we look at such a curve, it is spiralling away from us in either a clockwise or an anticlockwise fashion. In Fig. 9, the red curve is spiralling away clockwise whether one looks from above or from below, but the blue curve (once when grasps its position relative to the red one) is fleeing anticlockwise. The sign of the torsion represents the "chirality" of the curve, which is reversed when one forms the mirror image.

Now any curve in space has a motion that approximates a spiral, unless it is moving instantaneously in a plane, at which point its torsion will be exactly zero. In Fig. 9, this happens at the single base point separating the red and blue parts of the curve. One can apply the same principle to any space curve, and Fig. 10 displays a single trajectory of the Lorenz attractor coloured according to its chirality. The "null-torsion" points are those where the colour changes, and by considering all trajectories simultaneously filling out space, one might imagine that the totality of such points forms a 2-dimensional surface.

The functions $K(s)$ and $\tau(s)$ crop up in the so-called Serret-Frenet equations that enable one to define and differentiate a triad of unit mutually perpendicular unit vectors at each point of a space curve. This is a topic covered in every introductory textbook to differential geometry, and we refer the reader to, for example, [3–5].

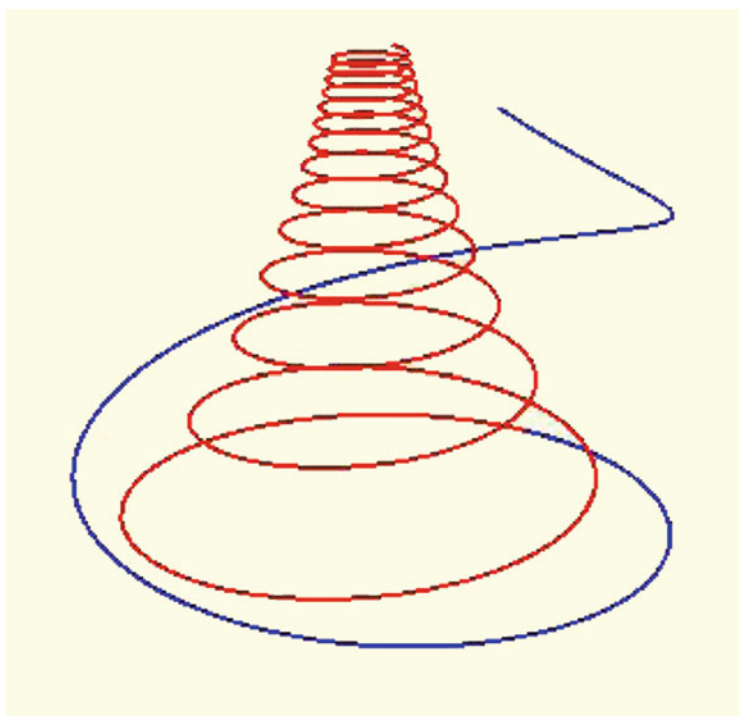


Fig. 9 The chirality of spirals

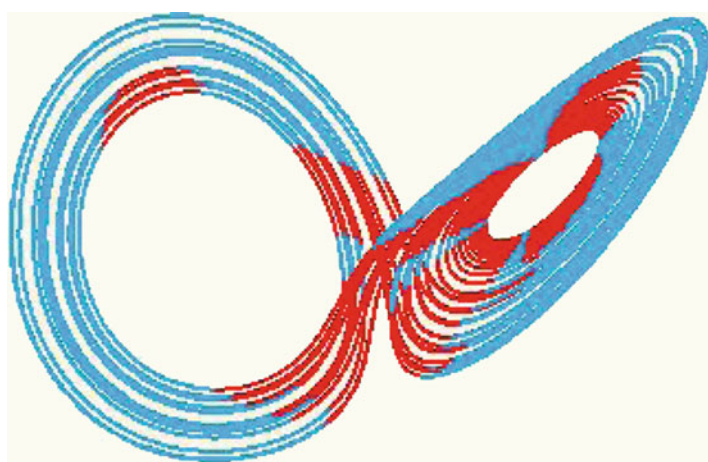


Fig. 10 Lorenz attractor coloured by torsion

4 The Torsion of a Vector Field

A key point that is not normally explained in standard texts is that the quantities curvature K and torsion τ can be defined at every point in space, once one is given a vector field V , which consists of assigning an arrow to every point in space. In practice, the arrows are specified by their Cartesian coordinates, as in the example

$$V = (10y - 10x, -xz + 28x - y, xy - 3z) \quad (1)$$

that gives rise to (a slightly simplified version of) the attractor discovered by Edward Lorenz, to approximate the Navier-Stokes equations that govern fluid flow in meteorology. It is not very useful to plot a selection of the arrows, though this is done in Fig. 11, in which the black dots represent the three points

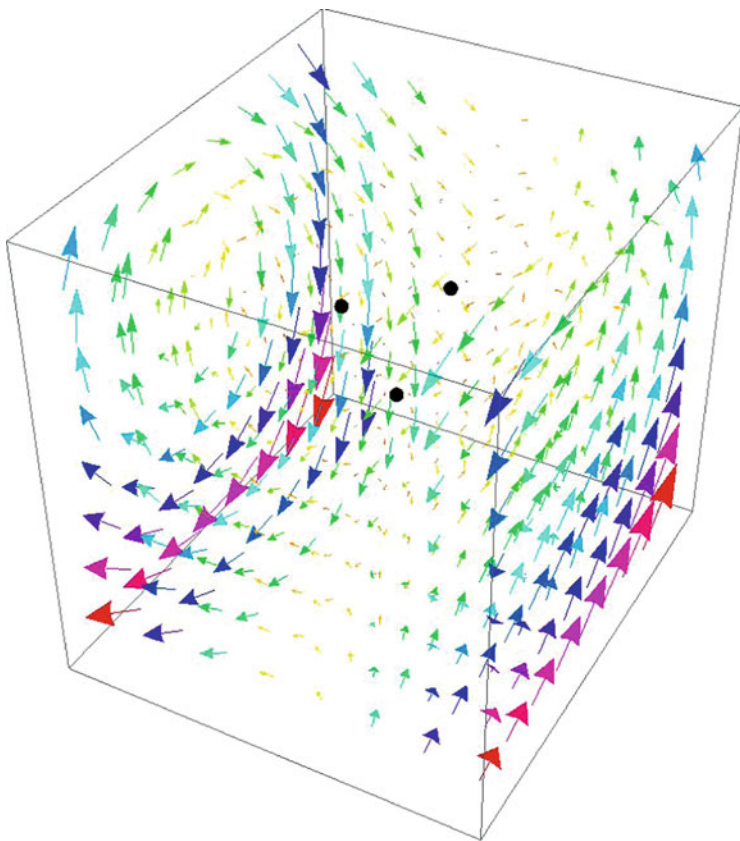


Fig. 11 A vector field of arrows

$$(0, 0, 0), \quad (9, 9, 27), \quad (-9, -9, 27),$$

where the three components of V are simultaneously equal to zero.

Starting from any point (apart from a black dot), one can in theory follow the arrows and generate a unique trajectory. It is more interesting to visualize families of trajectories, like the one in Fig. 10. In this way, the vector field gives rise to a family of spaces curves that never touch one another. (The vector field is allowed to be zero at one or more points; at such points the arrow has zero length, no curve passes through the point, and strictly speaking neither K nor τ have a value there.) Whilst the typical trajectory is infinite in length, it is known that certain trajectories are actually closed curves or knots of varying complexity [1].

We can see from the definition of V on the previous page that a vector field is specified by giving three functions, each of three variables. It is an easy matter to compute the curvature and torsion by computer from an explicit knowledge of such functions. It requires computing two derivatives of the components of V , and then combining them in a highly non-linear fashion. Figure 12 is output from the program *Mathematica* expressing the torsion of the Lorenz vector field V . The details are unimportant, but it is worth noting that the equation itself is not at all elegant. Instead it is the definition or algorithm that leads to this output that is elegant.

If we set the quantity in Fig. 12 equal to zero, we obtain the "null-torsion" surface of Fig. 1 consisting of points where the torsion of V is zero. Actually, that is not quite true, there are other points with zero torsion not shown—namely those lying on the z -axis $x = 0 = y$, which is itself a trajectory of the Lorenz field. The surface is one component of the variety of degree 8 defined by the vanishing torsion. More vivid views of the null-torsion surface (with trajectories) can be seen in Figs. 13 and 14, and another in Fig. 15.

One can think of the Fig. 14 as representing a "stand" that could be placed on an office desk in order to properly display the more famous Lorenz curves. The second "upside-down" view better displays the self-intersections of the surface, and a key feature of it, namely that it incorporates two "leaves" that are roughly planar (in

$$\begin{aligned} & x^6 y^2 + x^6 z^2 - 56 x^6 z + 784 x^6 - 2 x^5 y z - 112 x^5 y + 20 x^4 y^2 z - \\ & 558 x^4 y^2 + 20 x^4 z^3 - 1678 x^4 z^2 + 48944 x^4 z - 486864 x^4 - 30 x^3 y^3 z + \\ & 480 x^3 y^3 - 30 x^3 y z^3 + 2140 x^3 y z^2 - 53164 x^3 y z + 492912 x^3 y + \\ & 570 x^2 y^4 + 600 x^2 y^2 z^2 - 29760 x^2 y^2 z + 344817 x^2 y^2 - 30 x^2 z^4 + \\ & 2460 x^2 z^3 - 70623 x^2 z^2 + 666792 x^2 z - 300 x y^5 - 300 x y^3 z^2 + \\ & 16870 x y^3 z - 244080 x y^3 + 270 x y z^3 - 13140 x y z^2 + 214326 x y z + \\ & 100 y^4 z + 13500 y^4 - 300 y^2 z^3 + 15480 y^2 z^2 - 238140 y^2 z \end{aligned}$$

Fig. 12 A polynomial of degree eight

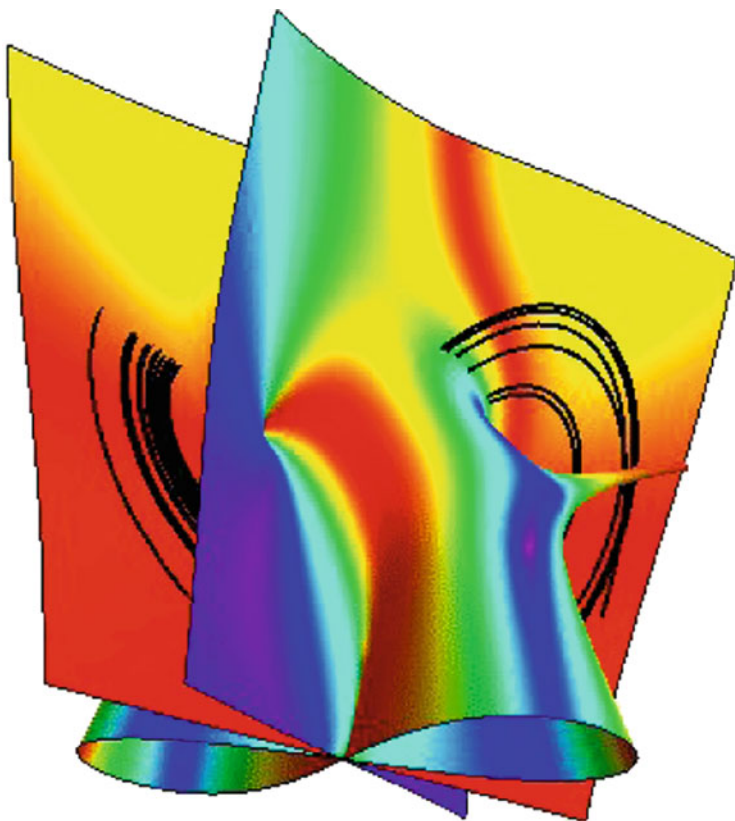


Fig. 13 Lorenz stand

theory these extend to infinity but of course we are only plotting part of the surface). One can understand this feature as follows. Roughly speaking, the butterfly attractor does itself fit into two planes that intersect at an acute angle (this is best seen in Fig. 10). If this were exactly true then all the points on the corresponding planar trajectories would have zero torsion (recall that τ measures the extent to which a curve does not lie in a plane).

The colours of Figs. 14 and 15 have a precise mathematical meaning. The spectrum (Red–Orange–Yellow–Green–Blue–Indigo–Violet) is used to indicate the angle with which the trajectories following the vector field emerge from the surface. Red indicates that they are tangent, so if the two leaves were exact planes they would be painted red all over. At the opposite extreme, violet represents points where the trajectories emerge at right angles (visible on subsequent images). Green would represent roughly a 45° angle of incidence between surface and curve.

Another aspect of the surface, more evident in the versions of Figs. 1 and 15, is the presence of cusps that form at two of the three points where the vector field

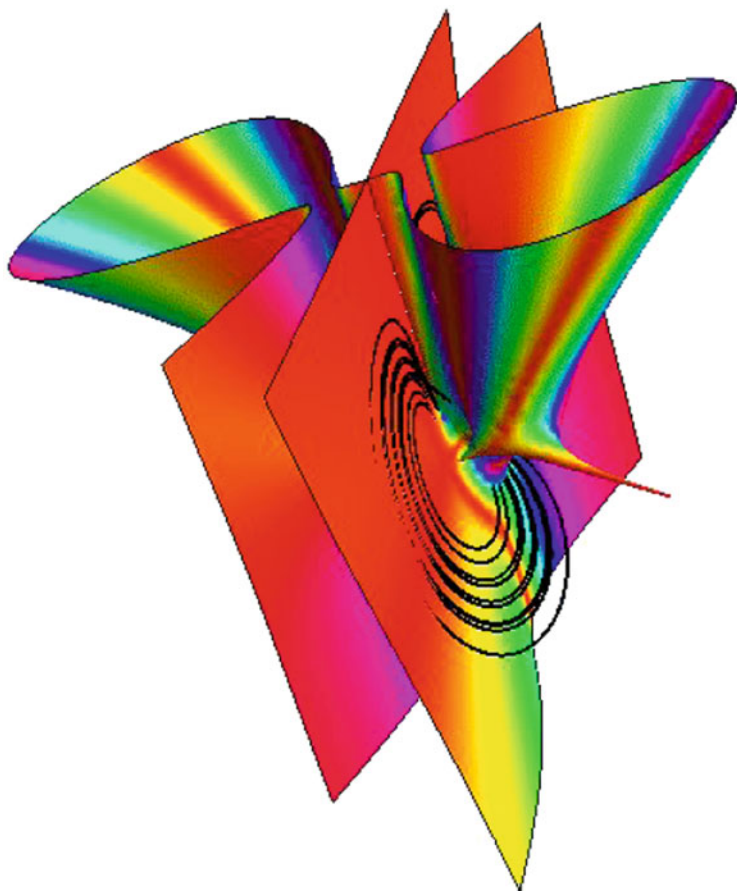


Fig. 14 Inverted stand revealing self-intersections

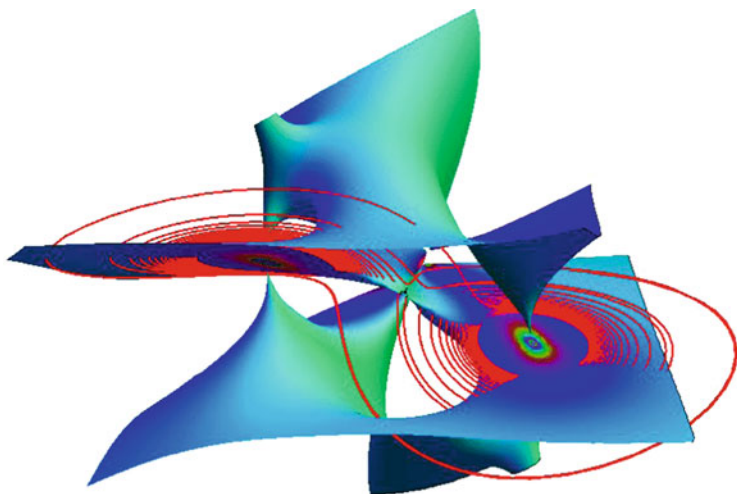


Fig. 15 Null-torsion surface coloured by curvature

is zero (physically, these can be thought of as equilibrium points of the dynamical system). Near these two points, the surface resembles a double cone (whose vertex is the respective point) separated by a plane. Actually, the surface is singular at all three such points, although the nature of the singularity at the origin is more complicated. What is perhaps more surprising is the presence of external spikes, though these point to the behaviour of other trajectories that are not shown.

Although the blue-green surface of Fig. 15 is also defined by setting the polynomial in Fig. 13 equal to zero, its colouring is related to the non-negative curvature function K . The latter becomes infinite as one approaches the two equilibrium points.

5 A Gallery of Null-Torsion Surfaces

Having mastered the manner in which the surfaces on the previous pages were constructed from the data defining the vector field V , it is an easy matter to apply the technique (and in practice, the computer program) to obtain other images. Above all, it is remarkable how much varied behaviour one encounters by restricting to quadratic vector fields, namely those component functions are polynomials of degree at most two. There is a degree of classification of the physically-relevant dynamical systems that arise from such fields in [2]. As explained there, one of the deceptively simplest examples is the vector field

$$W = (-y - z, x + \frac{1}{2}y, 2 + xz - 4z),$$

defined by the biochemist Otto Rössler (also a recent critic of the LHC). Notice that only the third component is quadratic—the first two are linear. Its associated trajectories form an analogue of a Möbius band (cf. Fig. 3) that is supported by its own version of the null-torsion surface, shown as Fig. 16 with a more autumnal colouring.

We shall briefly describe the images on the following page.

Figure 17 was chosen for its compact trajectories.

Figure 18 represents a null-torsion surface for a vector field close to the linear case, in which the torsion vanishes on a union of planes in space, intersecting at the origin.

The remaining two figures arise from the quadratic vector field

$$\begin{aligned} Q_a &= (1 + yz + ax^2, 1 + zx + ay^2, 1 + xy + az^2) \\ &= (1, 1, 1) + (yz, zx, xy) + a(x^2, y^2, z^2) \end{aligned} \tag{2}$$

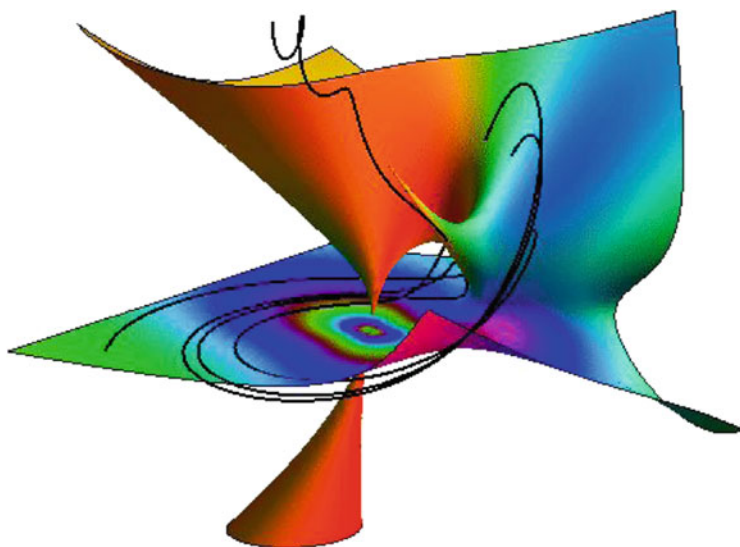


Fig. 16 Null torsion for the Rössler attractor

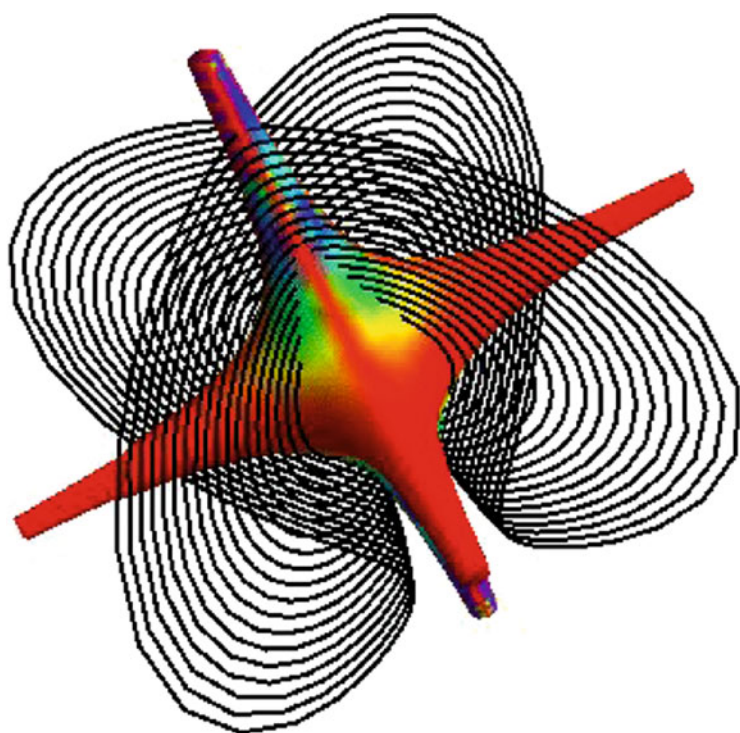


Fig. 17 Coiled trajectories

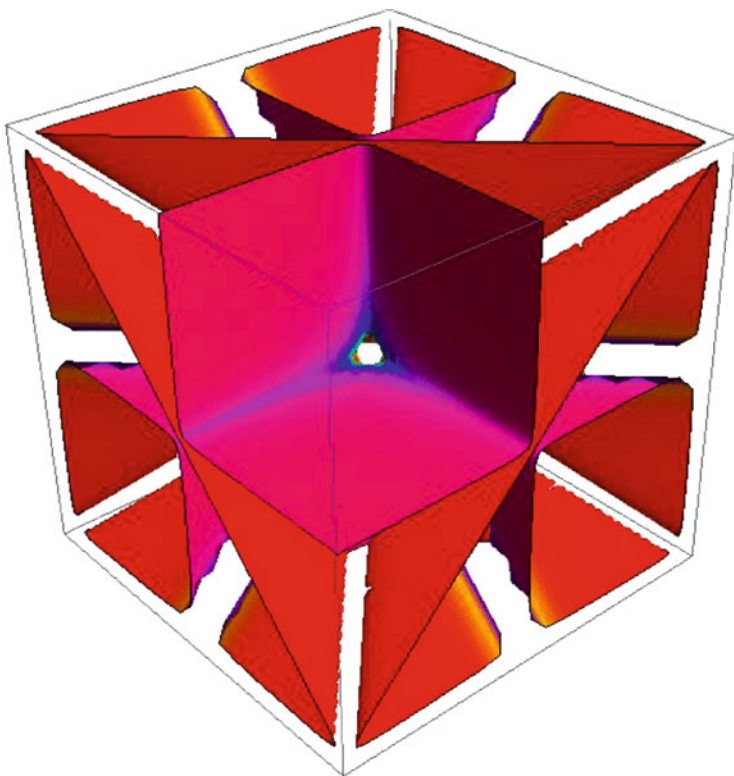


Fig. 18 Near-planar surface

for different values of the parameter a , Fig. 19 has $a = 1$ and Fig. 20 has $a = 1/4$. We explain below that the resulting vector fields have a threefold symmetry (this is more evident in Fig. 20).

On the next page, we display vanishing torsion arising from the vector field

$$(\sin y, \sin z, \sin x),$$

which is triply periodic since if we move a distance 2π in the x , y or z direction the value of the vector field remains the same. Figure 21 displays the associated null-torsion surface, coloured as in Figs. 13 and 14. Figure 22 is a view of one "cube" of the surface with some associated trajectories, which we see spiralling in the centre of the picture so as to arrive tangent to the red zone.

The vector fields giving rise to the previous images all possess a certain degree of symmetry, characterized by the action of some group of transformations that leave the equations invariant. For example, the Lorenz field V defined by (1) is unchanged when the signs of both x and y are reversed. This represents invariance by a 180° rotation around the z axis, which incidentally identifies two of the three

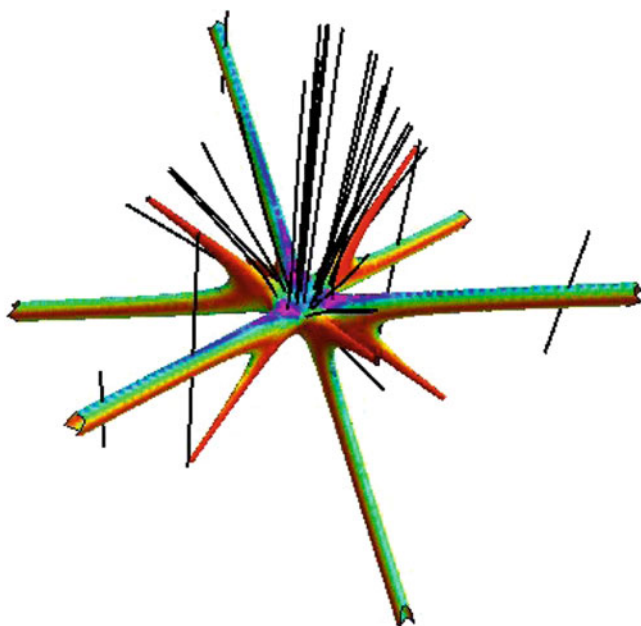


Fig. 19 Quadratic case Q_1

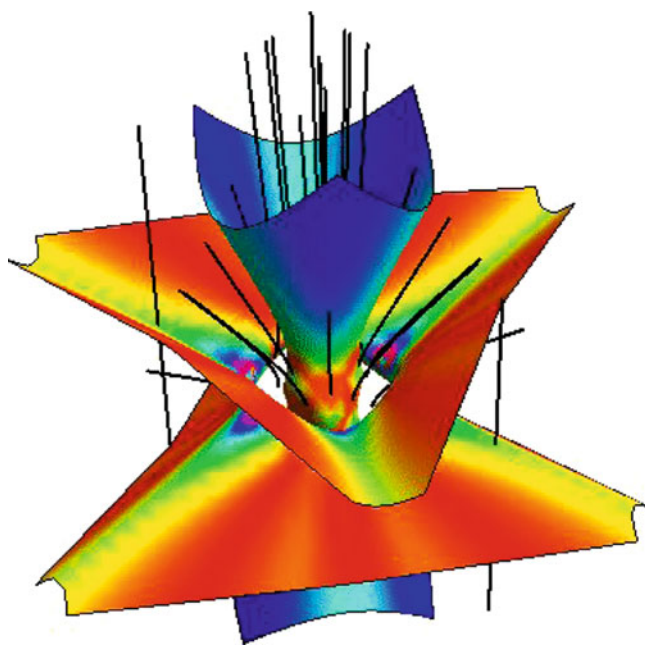


Fig. 20 Quadratic case $Q_{1/4}$

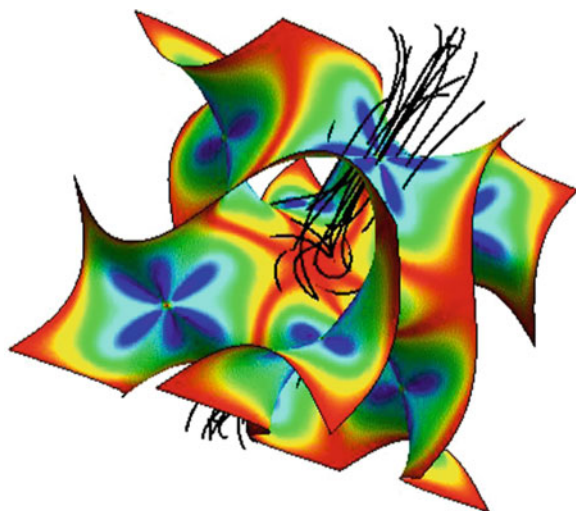


Fig. 21 A triply periodic surface

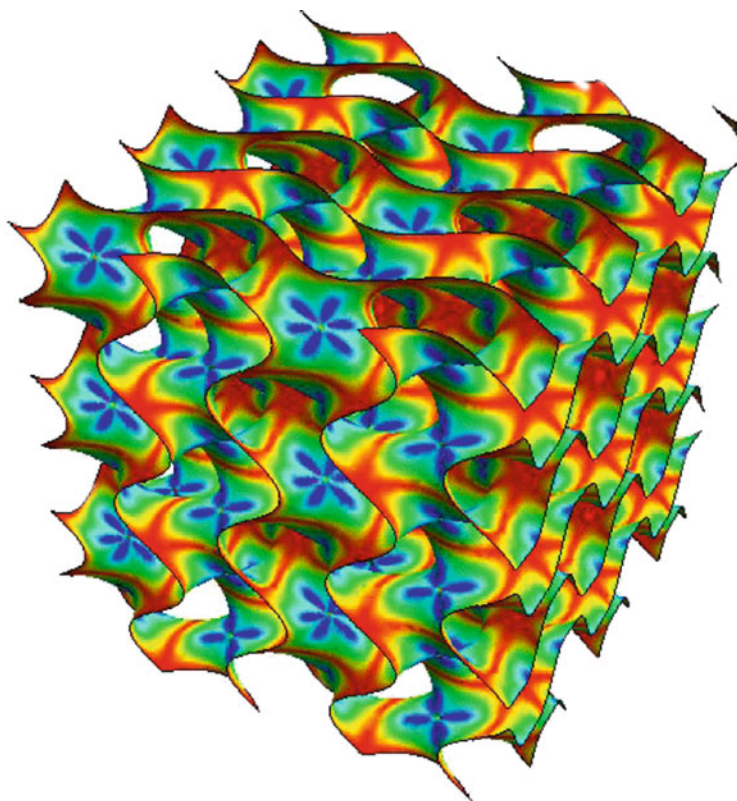


Fig. 22 Detail with sinusoidal trajectories

equilibrium points. For the sinusoidal figures, the group consists of translations defined by a lattice in space.

The symmetry realized by the vector field Q_a of (2) is threefold. To explain this, let ρ denote a rotation of 120° about the axis $(1,1,1)$ —this is simply the linear transformation of \mathbb{R}^3 that cyclically permutes the coordinates:

$$\rho(x, y, z) = (y, z, x).$$

Then for each fixed a , the vector field Q_a has the property that (as a function $\mathbb{R}^3 \rightarrow \mathbb{R}^3$) it commutes with ρ :

$$Q_a(y, z, x) = \rho(Q_a(x, y, z)).$$

A consequence of this is that the "tri-rotation" ρ maps each trajectory of Q_a onto another trajectory.

Figures 23 and 24 arise from the vector field Q_a in (2) with $a = -1$. For this unique value of the constant a , the torsion is identically zero, and the

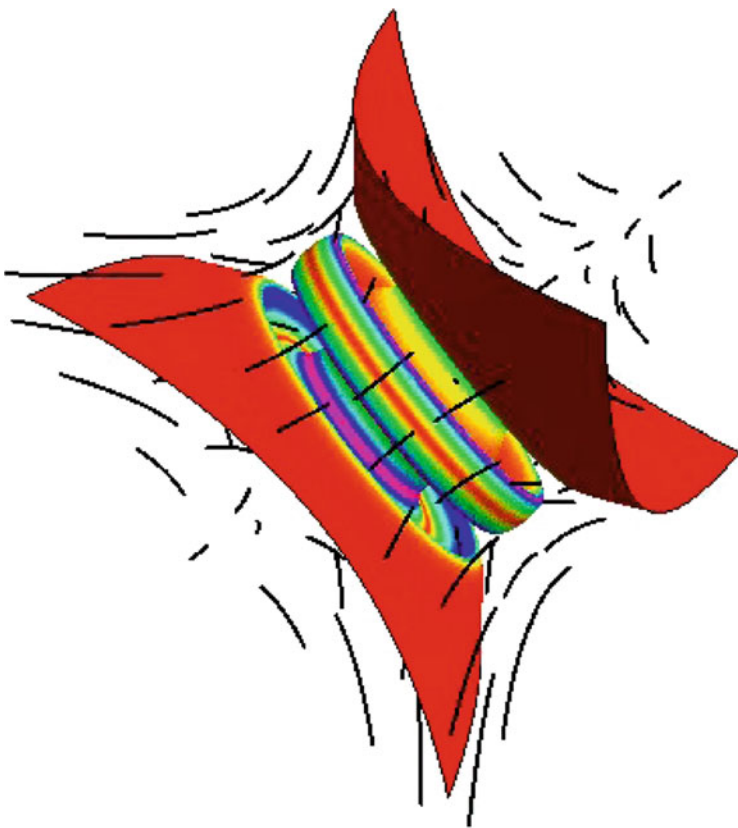


Fig. 23 Gas-ring necklace

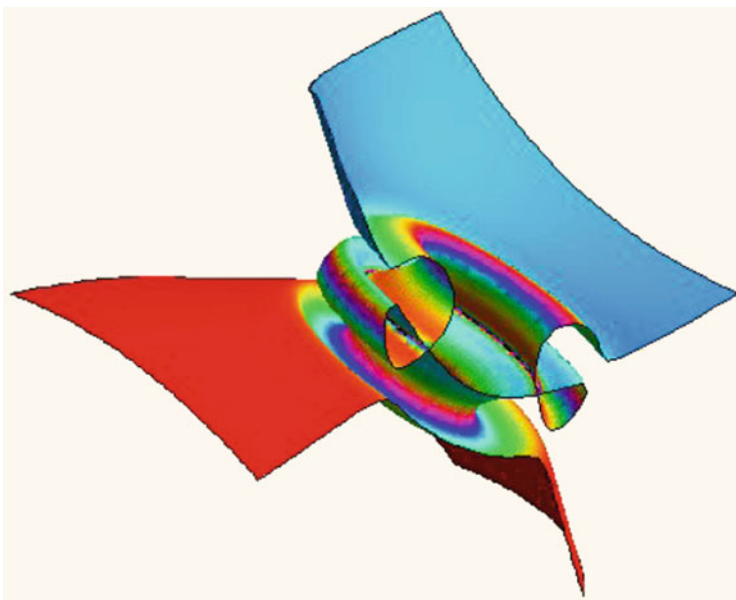


Fig. 24 Cut-away view

resulting vector field Q_{-1} has a continuous symmetry. Any one trajectory lies in a plane, but there is a rotational symmetry as this plane is allowed to rotate around the axis $(1,1,1)$. It turns out that one can factor out by the terms that makes the torsion zero, so as to plot the points where the torsion vanishes to second order. The result is the "gas-ring necklace" of Fig. 23. The smaller Fig. 24 is (despite a different colour scheme) a cut-away view to expose the neat self-intersection.

An obvious generalization of Q_{-1} is the vector field

$$(1 + yz - x^3, 1 + zx - y^3, 1 + xy - z^3). \quad (4)$$

This has cubic coefficients and the associated null-torsion surface is shown in Fig. 25 on the last page of this article.

Acknowledgments I first started using iterated exponentiation to illustrate bifurcation in a project for a Maple course I taught in Oxford in the 1990s. Remnants of this course are available on my homepage.

The study of space curves with assigned torsion and curvature is described in [3], and I used it as a student competition to find an interesting space curve by guessing simple candidate functions in a differential geometry course in Turin.

The vector field Q_a is the basis of the author's animation

Vector field Kaleidoscope on YouTube. This video contains frames of null-torsion surfaces for about 500 values of a and Figs. 19, 20 and 23 are instances of that.

Figure 25 arises from the vector field (4) with cubic components. As personal computing power increases, it will be easier to study more and more complicated vector fields and their associated surfaces.

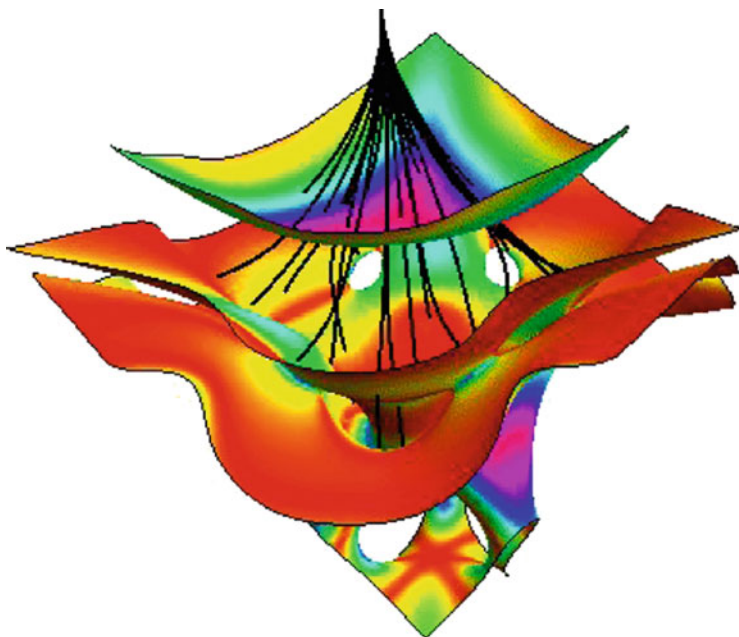


Fig. 25 Illustrating the geometry inherent in a cubic vector field

The ESMA conference taught me not just to better appreciate artistic aspects inherent in modern mathematics, and but also the importance of explaining to a wider public the underlying geometrical ideas I deal with on a daily basis. I found myself having to work on a number of deep mathematical problems to answer some of the questions that arose. In this respect, I wish to express gratitude to the participants, and in particular François Apery, Claude Bruter, Eugenia Emets, George Hart, and Jos Leys. Thanks are also due to Claude for his afternoon visits from Gometz to Bures encouraging me to finish the text.

References

1. Ghys, E.: Lorenz and modular flows, a visual introduction, www.ams.org/samplings/feature-column/fcarc-lorenz
2. Gilmore, C.R., Letellier, C.: The Symmetry of Chaos. Oxford University Press, London (2007)
3. Gray, A., Abbena, E., Salamon, S.: Modern Differential Geometry of Curves and Surfaces with Mathematica. CRC Press, FL (2006)
4. Pressley, A.: Elementary Differential Geometry, Springer Undergraduate Mathematics Series. Springer, Berlin (2001)
5. Struik, D.: Lectures on Classical Differential Geometry. Dover, NY (1988)

Mathematics and Modern Art

Proceedings of the First ESMA Conference, held in
Paris, July 19-22, 2010

Bruter, C. (Ed.)

2012, VIII, 178 p., Hardcover

ISBN: 978-3-642-24496-4